Advanced Steel Construction – Vol. 18 No. 2 (2022) 585–591
DOI:10.18057/IJASC.2022.18.2.7

AN INNOVATIVE CABLE ELEMENT ALLOWING FOR SLIDING EFFECT

Jian-Wei He [1], De-Hong Huang [2], Yao-Peng Liu [1, 2, 3, *], Wen-Feng Chen [1], Yue-Yang Ding [1] and Siu-Lai Chan [1]

[1] *Department of Civil and Environmental Engineering, The Hong Kong Polytechnic University, Hong Kong, China*
[2] *School of Civil Engineering, Southwest Jiaotong University, Chengdu, China*
[3] *NIDA Technology Company Limited, Hong Kong, China*
** (Corresponding author: E-mail: yaopeng.liu@connect.polyu.hk)*

ABSTRACT

Sliding motion has attracted much attention in the design of cable structures such as flexible barriers and suspend-dome structures. Engineers can take the benefit of sliding behavior to develop the innovative cable systems like flexible barriers to absort large impact energy while the risk of sliding in some cable dome structures should be evaluated. The conventional analysis methods need many straight-line cable elements but with inaccurate results and low numerical efficiency. The well-known catenary cable element show high performance in the cable structures but limited to no sliding cases. Thus, an advanced cable element allowing for sliding effect is urgently required in the practical analysis of cable structures. In this paper, a super cable element based on the conventional catenary cable element is proposed to model the segments within a slidable cable. In the proposed super element, every segment performs in the characteristic of catenary cable. Meanwhile, the sliding motion will be activated when the unbalanced axial force between segments are deteced and as a result, the sliding behaviours of the cables in both taut and slack states can be modelled. This work has not been done in previous research and the proposed element can be applied to many structures. The verification examples show the accuracy and efficiency of the proposed element in the analysis of cable structures with internal movement passing the supports or relocation of the loading points.

ARTICLE HISTORY

Received: 6 May 2021
Revised: 8 October 2021
Accepted: 20 November 2021

KEYWORDS

Cable structures;
Flexible barrier system;
Sliding behavior;
Catenary cable element;
Multi-node cable element

1. Introduction

Cable systems are widely used in many structures. The primary advantage of cable structures is that they are of light weight but with high strength. Furthermore, the cables can be easily adjusted to suit the structural shapes and form optimal load paths due to high flexibility. These features make them applicable in many different kinds of structures such as flexible barriers (Coulibaly et al., 2018; Yu et al., 2018; L. Zhao et al., 2020; Lei Zhao et al., 2020), transmission lines (Aufaure, 1993, 2000), pulley system (Ju and Choo, 2005), suspend-dome structures (Chen et al., 2010), clustered tensegrity (Kan et al., 2018), and parachute systems (Zhou et al., 2004).

Recently, one type of protection structures named flexible barrier is adopted in the interception of debris flows and rockfalls. Generally, this flexible barrier system consists of steel cables, ring nets, steel posts, and energy dissipation devices. Different from the traditional rigid barriers with large geometric sizes and masses such as embankments and rock shed, this type of protection structure exhibits its capability to stop rockfalls and debris flows through its large deflections to absort the impact energy. During the impact process, rockfalls and debris flows are retarded by the barrier via the large deflection of the cables and the sliding motion between the ring nets and cables. For a typical flexible barrier, the ring nets are attached to the support cables which are suspended spanning the steel posts with their ends anchored to the ground. The ring nets can move along the cable while the cable can slide passing through the joints on the steel post. According to the study on the mechanism of such systems subjected to impact of rockfalls or debris flows, the efficiency of the sliding motion of the cables contributes to the successful performance of the whole system (Yu et al., 2018). The mechanism of sliding cables can be also found in other systems such as pulley systems, clustered tensegrity, suspend-dome structure, parachute systems. In such systems, cables are also allowed to slide passing through the joints.

Several methods have been proposed to conduct the analysis of cable structures allowing for sliding motion.

In most of the methods, the segments in a sliding cable are assumed to be straight-line in the analysis. In general, the methods can be classified into two types based on the node numbers involved in the sliding cable element. The first type of the sliding cable element consists of three nodes and two cable segments. Aufaure (1993, 2000) developed this element to account for pulleys in the transmission line system, in which the intermediate node representing the pulley can only move within the total length of the element. However, this element is limited in the sliding case with multiple intermediate nodes. Zhou et al. (2004) raised another sliding cable element based on the same assumption with the previous method that the strain was uniform along the element but classified a string of cable into the active and inactive sliding portions, respectiely. In their work, a searching algorithm was introduced to identify the active and inactive sliding portions in every iteration. This method made it possible to adopt the three-node element in multi-node sliding analysis. LSTC (2019) introduced a sliprings element, which required an additional slipring node coincident with the intermediate node of the two cable segments. The slip at the slipring node was calculated from the ratio of the forces at the two elements. A remeshing algorithm was also proposed to allow more elements passing through the slipring. Ju and Choo (2005) proposed a multi-node sliding cable element without use of searching algorithm and remeshing method. To overcome the problem in the multiple pulleys system, a super element was presented where the passages over the pulleys were adapted as variables based on the translational nodal displacements. The sliding criteria of the cable was governed by the force difference at two adjacent sub-elements. Chen et al. (2010) extended the method proposed by Zhou et al. (2004) from three-node element to multi-node element. Their element was successfully applied to the analysis of a suspen-dome structure with multi-node sliding case.

Two different sliding criteria can be found from the previous research. The first one is that the strain along the cable element remains constant, which ensures the continuity of the elongation and the tensile force of the sliding cable. The principle of virtual work can be adopted to derive the element stiffness. Generally, the sliding cable segment is assumed to be straight-line when adopting this criterion. The segment length equals to the distance between the segment end nodes. The coordinates of the nodes are updated through the interation process. Subsequently, the segment length is adjusted due to the displacement of the nodes. Hence, the sliding motion of the cable element is achieved by adjusting the segment lengths while the nodes are relocated to the new equilibrium state (Chen et al., 2010; Kan et al., 2018). However, due to the assumption of constant strain along the element, the tensile forces in any segments of the sliding cable are subsequently constant. The other criterion is that sliding motion is determined by the force relationship at any sliding joint between two adjacent cable segments (Ju and Choo, 2005; LSTC, 2019). Once the unbalanced force is detected, the cable will slide passing through the joint. The relationship among the cable segments and the joint is clear while the friction between the cable segments and the joints can be easily assembled into the system. In contrast to the first criterion, the tensile forces in the segments might be different in the second method, in which only the continuity at the sliding joint is stipulated.

In the aforementioned methods, the cable segment is represented using straight-line element. However, the straight-line element cannot well describe the actual geometry configuration of cables due to the nature of flexibility, especially for the cable with large sag. Thus, the model by using straight-line sliding cable elements cannot simulate the slide motion accurately. When extensive elements are used to model the sag effect, it will lead to siginificant increase of modelling complexity and computer time with numerical convergent problems. Hence, some researchers adopted catenary element to model the behaviour of cables (Salehi Ahmad Abad et al., 2013; Thai and Kim, 2011). Unlike the straight-line elements, this method takes the catenary nature of the cable into consideration. The axial forces along the cable segments need not be constant and the sag of the segments can be well captured. Generally speaking,

the real geometry configuration and axial force distribution of the cable with small and large sag can be well represented. However, there are still limited works on modelling of sliding motion by catenary cable element allowing for several internal nodes.

In this paper, a super cable element based on the conventional catenary cable element is proposed to model the segments within a slidable cable. In the proposed super element, every segment performs in the characteristic of catenary cable. Meanwhile, the sliding motion will be activated when the unbalanced axial force between segments are deteced and as a result, the sliding behaviours of the cables in both taut and slack states can be modelled. This work has not been done in previous research and the proposed element can be applied to many structures such as flexible barriers, transmission towers, pulley system, suspend-dome structures, clustered tensegrity and parachute systems.

When the sliding behaviour of the cable is allowed, the increment of axial force on the cable should be not too large so that the geometry adjustment of the cable segments can be successfully carried out to find a new force equilibrium position. Note that the cable segments are generally in the elastic state due to the length adjustment. Hence, the sliding cable element is assumed to be elastic all the time in this paper.

2. Formulations of conventional catenary cable element

The assuptions adopted in the elastic catenary cable element include:

1. The cable is perfectly flexible;
2. The cross-sectional area of cable is contant;
3. The cable is linear elastic;
4. The cable is subjected to distributed loads and thermal action.

The general catenary cable is showed in Figure 1. A cable is suspended between two end nodes with a unstrained length of l_0. The end nodes have the Cartesian ordinates $(0,0,0)$ and (l_x, l_y, l_z). The Lagrangian coordinate of any position in the cable is described by s and p in the unstrained and strained profile. The geometric constraint of the cable is given by:

$$\left(\frac{dx}{dp}\right)^2 + \left(\frac{dy}{dp}\right)^2 + \left(\frac{dz}{dp}\right)^2 = 1 \tag{1}$$

Further, the equilibrium of the cable in three dimensions can be expressed as:

$$T\left(\frac{dx}{dp}\right) = -f_x - w_x s \tag{2}$$

$$T\left(\frac{dy}{dp}\right) = -f_y - w_y s \tag{3}$$

$$T\left(\frac{dz}{dp}\right) = -f_z - w_z s \tag{4}$$

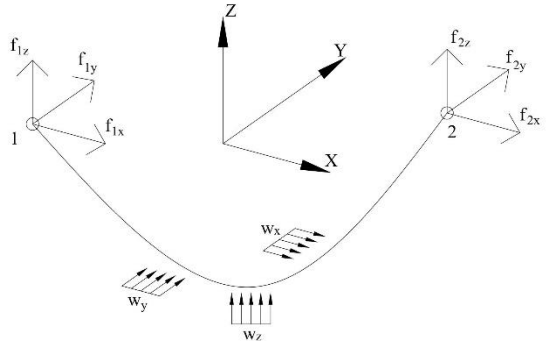

Figure 1. Coordinate System of a Catenary Cable Element

In accordance with the Hook's law, the constitutive relation of the cable can be expressed as:

$$T = EA(\frac{dp}{dx} - 1 - \alpha\Delta T) \tag{5}$$

where E is the elastic modulus; A is the cross-sectional area; α is the thermal expansion coefficient and ΔT is the temperature change.

The distance of any position in the cable can be expressed using the unstrained length:

$$x(s) = \int_0^s dx = \int_0^s \frac{dx}{dp}\frac{dp}{ds}\, ds \tag{6}$$

$$y(s) = \int_0^s dy = \int_0^s \frac{dy}{dp}\frac{dp}{ds}\, ds \tag{7}$$

$$z(s) = \int_0^s dz = \int_0^s \frac{dz}{dp}\frac{dp}{ds}\, ds \tag{8}$$

Hence, the projected length between two end nodes can be derived from the above equations when $s = l_0$.

$$l_i = -\frac{f_{1i}l_0}{EA} - \frac{w_i l_0^2}{2EA} + \frac{1+\alpha\Delta T}{w^3}\Big[ww_i\left(\sqrt{\sum(f_{1i})^2} - \sqrt{\sum(w_i l_0 + f_{1i})^2}\right) + (w^2 f_{1i} - Sw_i)\left(ln\left(\frac{S}{w} + \sqrt{\sum(f_{1i})^2}\right) - ln\left(wl_0 + \frac{S}{w} + \sqrt{\sum(w_i l_0 + f_{1i})^2}\right)\right], \quad i = x, y, z \tag{9}$$

$$w = \sqrt{w_x^2 + w_y^2 + w_z^2} \tag{10}$$

$$S = f_x w_x + f_y w_y + f_z w_z \tag{11}$$

To solve the equations above using an iterative technique, the incremental relationship between the projected length and the nodal force can be established:

$$\begin{bmatrix} dl_x \\ dl_y \\ dl_z \end{bmatrix} = \begin{bmatrix} \frac{\partial l_x}{\partial f_{1x}} & \frac{\partial l_x}{\partial f_{1y}} & \frac{\partial l_x}{\partial f_{1z}} \\ \frac{\partial l_y}{\partial f_{1x}} & \frac{\partial l_y}{\partial f_{1y}} & \frac{\partial l_y}{\partial f_{1z}} \\ \frac{\partial l_z}{\partial f_{1x}} & \frac{\partial l_z}{\partial f_{1y}} & \frac{\partial l_z}{\partial f_{1z}} \end{bmatrix} \begin{bmatrix} df_{1x} \\ df_{1y} \\ df_{1z} \end{bmatrix} = \boldsymbol{F} \begin{bmatrix} df_{1x} \\ df_{1y} \\ df_{1z} \end{bmatrix} \tag{12}$$

in which, $\boldsymbol{F}$ is the flexibility matrix of the element. The components in the flexibility can be calculated by:

$$\frac{\partial x_i}{\partial f_{1i}} = -\frac{l_0}{EA} + \frac{1+\alpha\Delta T}{w^3}\Big[ww_i\left(\frac{f_{1i}}{T_1} - \frac{w_i l_0 + f_{1i}}{T_2}\right) + (w^2 - w_i^2)\left(ln\left(\frac{S}{w} + T_1\right) - ln\left(wl_0 + \frac{S}{w} + T_2\right)\right) + (w^2 f_{1i} - Sw_i)\left(\frac{w_i T_1 + wf_{1i}}{T_1(S + wT_1)} - \frac{w_i T_2 + w(f_{1i} + w_i l_0)}{T_2(w^2 l_0 + S + wT_2)}\right)\Big] \tag{13}$$

$$\frac{\partial x_i}{\partial f_{1j}} = \frac{1+\alpha\Delta T}{w^3}\Big[ww_i\left(\frac{f_{1j}}{T_1} - \frac{w_j l_0 + f_{1j}}{T_2}\right) + (-w_i w_j)\left(ln\left(\frac{S}{w} + T_1\right) - ln\left(wl_0 + \frac{S}{w} + T_2\right)\right) + (w^2 f_i - Sw_i)\left(\frac{w_j T_1 + wf_{1j}}{T_1(S + wT_1)} - \frac{w_j T_2 + w(f_{1j} + w_j l_0)}{T_2(w^2 l_0 + S + wT_2)}\right)\Big] \tag{14}$$

$$T_1 = \sqrt{\sum(f_{1i})^2} \tag{15}$$

$$T_2 = \sqrt{\sum(w_i l_0 + f_{1i})^2} \tag{16}$$

where, $i = x, y, z; j = x, y, z; i \neq j$.

To incorporate the cable element to the conventional stiffness-based program, its tangent stiffness matrix $\boldsymbol{K}$ can be obtained by inversing the flexibility matrix $\boldsymbol{F}$:

$$\boldsymbol{K} = \boldsymbol{F}^{-1} \tag{17}$$

3. Formulations of sliding catenary cable element

To account for the sliding effect, the slip distance of the cable at the nodes are taken as one of variables in the element.

Figure 2 shows the proposed sliding catenary cable element. The slip distances at the two end nodes are Δ_1 and $\Delta 2$. The total length difference of the cable is dl_0.

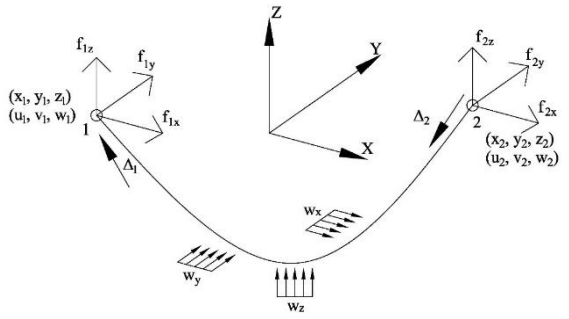

Figure 2. Configuration of the Proposed Sliding Catenary Cable Element

The relationship between the end forces of the end nodes can be expressed as:

$$f_{2i} = -f_{1i} - w_i l_0\,, \ (i = x, y, z) \tag{18}$$

The differential projected length of the cable as well as the unstrained length are given by:

$$\begin{bmatrix} dl_x \\ dl_y \\ dl_z \\ dl_0 \end{bmatrix} = \begin{bmatrix} u_2 - u_1 \\ v_2 - v_1 \\ w_2 - w_1 \\ \Delta_2 - \Delta_1 \end{bmatrix} \tag{19}$$

where, u, v, w are the displacements of the nodes.

In addition to the equilibrium equations of ordinary catenary cable element, an additional equation is required to establish the equilibrium of the tension forces at a node in the continuous cable. To account for the tension force in a catenary cable element, the stiffness matrix of the element can be extended as follow:

$$\begin{bmatrix} df_{1x} \\ df_{1y} \\ df_{1z} \\ dT_1 \end{bmatrix} = \begin{bmatrix} \frac{\partial f_{1x}}{\partial l_x} & \frac{\partial f_{1x}}{\partial l_y} & \frac{\partial f_{1x}}{\partial l_z} & \frac{\partial f_{1x}}{\partial l_0} \\ \frac{\partial f_{1y}}{\partial l_x} & \frac{\partial f_{1y}}{\partial l_y} & \frac{\partial f_{1y}}{\partial l_z} & \frac{\partial f_{1y}}{\partial l_0} \\ \frac{\partial f_{1z}}{\partial l_x} & \frac{\partial f_{1z}}{\partial l_y} & \frac{\partial f_{1z}}{\partial l_z} & \frac{\partial f_{1z}}{\partial l_0} \\ \frac{\partial T_1}{\partial l_x} & \frac{\partial T_1}{\partial l_y} & \frac{\partial T_1}{\partial l_z} & \frac{\partial T_1}{\partial l_0} \end{bmatrix} \begin{bmatrix} dl_x \\ dl_y \\ dl_z \\ dl_0 \end{bmatrix} = \begin{bmatrix} \boldsymbol{k}_{1fu,3x3} & \boldsymbol{k}_{1fl,3x1} \\ \boldsymbol{k}_{1tu,1x3} & \boldsymbol{k}_{1tl,1x1} \end{bmatrix} \begin{bmatrix} dl_x \\ dl_y \\ dl_z \\ dl_0 \end{bmatrix} \tag{20}$$

$$\begin{bmatrix} df_{2x} \\ df_{2y} \\ df_{2z} \\ dT_2 \end{bmatrix} = \begin{bmatrix} \frac{\partial f_{2x}}{\partial l_x} & \frac{\partial f_{2x}}{\partial l_y} & \frac{\partial f_{2x}}{\partial l_z} & \frac{\partial f_{2x}}{\partial l_0} \\ \frac{\partial f_{2y}}{\partial l_x} & \frac{\partial f_{2y}}{\partial l_y} & \frac{\partial f_{2y}}{\partial l_z} & \frac{\partial f_{2y}}{\partial l_0} \\ \frac{\partial f_{2z}}{\partial l_x} & \frac{\partial f_{2z}}{\partial l_y} & \frac{\partial f_{2z}}{\partial l_z} & \frac{\partial f_{2z}}{\partial l_0} \\ \frac{\partial T_2}{\partial l_x} & \frac{\partial T_2}{\partial l_y} & \frac{\partial T_2}{\partial l_z} & \frac{\partial T_2}{\partial l_0} \end{bmatrix} \begin{bmatrix} dl_x \\ dl_y \\ dl_z \\ dl_0 \end{bmatrix} = \begin{bmatrix} \boldsymbol{k}_{2fu,3x3} & \boldsymbol{k}_{2fl,3x1} \\ \boldsymbol{k}_{2tu,1x3} & \boldsymbol{k}_{2tl,1x1} \end{bmatrix} \begin{bmatrix} dl_x \\ dl_y \\ dl_z \\ dl_0 \end{bmatrix} \tag{21}$$

As shown in the equations, each stiffness matrix is composed of four components. The detail of the components are derived from the equations below:

a) $\boldsymbol{k}_{1fu,3x3}$ component

$$\boldsymbol{k}_{1fu,3x3} = \begin{bmatrix} \frac{\partial f_{1x}}{\partial l_x} & \frac{\partial f_{1x}}{\partial l_y} & \frac{\partial f_{1x}}{\partial l_z} \\ \frac{\partial f_{1y}}{\partial l_x} & \frac{\partial f_{1y}}{\partial l_y} & \frac{\partial f_{1y}}{\partial l_z} \\ \frac{\partial f_{1z}}{\partial l_x} & \frac{\partial f_{1z}}{\partial l_y} & \frac{\partial f_{1z}}{\partial l_z} \end{bmatrix} \tag{22}$$

$\boldsymbol{k}_{1fu,3x3}$ is the stiffness matrix of a general catenary cable element which can be determined from Eqs. (12) and (17).

b) $\boldsymbol{k}_{1fl,3x1}$ component

$$\boldsymbol{k}_{1fl,3x1} = \begin{bmatrix} \frac{df_{1x}}{dl_0} \\ \frac{df_{1y}}{dl_0} \\ \frac{df_{1z}}{dl_0} \end{bmatrix} = \begin{bmatrix} \frac{\partial f_{1x}}{\partial l_x} & \frac{\partial f_{1x}}{\partial l_y} & \frac{\partial f_{1x}}{\partial l_z} \\ \frac{\partial f_{1y}}{\partial l_x} & \frac{\partial f_{1y}}{\partial l_y} & \frac{\partial f_{1y}}{\partial l_z} \\ \frac{\partial f_{1z}}{\partial l_x} & \frac{\partial f_{1z}}{\partial l_y} & \frac{\partial f_{1z}}{\partial l_z} \end{bmatrix} \begin{bmatrix} \frac{\partial l_x}{\partial l_0} \\ \frac{\partial l_y}{\partial l_0} \\ \frac{\partial l_z}{\partial l_0} \end{bmatrix} = \boldsymbol{k}_{1fu,3x3} \begin{bmatrix} \frac{\partial l_x}{\partial l_0} \\ \frac{\partial l_y}{\partial l_0} \\ \frac{\partial l_z}{\partial l_0} \end{bmatrix} \tag{23}$$

$$\frac{\partial l_i}{\partial l_0} = -f_{2i}\left(\frac{1}{EA} + \frac{1+\alpha\Delta T}{T_2}\right), \tag{24}$$

$$T_2 = \sqrt{\sum (f_{2i})^2},\ i = x, y, z \tag{25}$$

c) $\boldsymbol{k}_{1tu,1x3}$ component

$$\boldsymbol{k}_{1tu,1x3} = \begin{bmatrix} \frac{\partial T_1}{\partial l_x} & \frac{\partial T_1}{\partial l_y} & \frac{\partial T_1}{\partial l_z} \end{bmatrix} = \begin{bmatrix} \frac{\partial T_1}{\partial f_{1x}} & \frac{\partial T_1}{\partial f_{1y}} & \frac{\partial T_1}{\partial f_{1z}} \end{bmatrix} \begin{bmatrix} \frac{\partial f_{1x}}{\partial l_x} & \frac{\partial f_{1x}}{\partial l_y} & \frac{\partial f_{1x}}{\partial l_z} \\ \frac{\partial f_{1y}}{\partial l_x} & \frac{\partial f_{1y}}{\partial l_y} & \frac{\partial f_{1y}}{\partial l_z} \\ \frac{\partial f_{1z}}{\partial l_x} & \frac{\partial f_{1z}}{\partial l_y} & \frac{\partial f_{1z}}{\partial l_z} \end{bmatrix}$$

$$= \begin{bmatrix} \frac{\partial T_1}{\partial f_{1x}} & \frac{\partial T_1}{\partial f_{1y}} & \frac{\partial T_1}{\partial f_{1z}} \end{bmatrix} \boldsymbol{k}_{1fu,3x3} \tag{26}$$

$$\frac{\partial T_1}{\partial f_{1i}} = \frac{f_{1i}}{T_1}, i = x, y, z \tag{27}$$

d) $\boldsymbol{k}_{1tl,1x1}$ component

$$\boldsymbol{k}_{1tl,1x1} = \frac{dT_1}{dl_0} = \begin{bmatrix} \frac{\partial T_1}{\partial f_{1x}} & \frac{\partial T_1}{\partial f_{1y}} & \frac{\partial T_1}{\partial f_{1z}} \end{bmatrix} \begin{bmatrix} \frac{\partial f_{1x}}{\partial l_x} & \frac{\partial f_{1x}}{\partial l_y} & \frac{\partial f_{1x}}{\partial l_z} \\ \frac{\partial f_{1y}}{\partial l_x} & \frac{\partial f_{1y}}{\partial l_y} & \frac{\partial f_{1y}}{\partial l_z} \\ \frac{\partial f_{1z}}{\partial l_x} & \frac{\partial f_{1z}}{\partial l_y} & \frac{\partial f_{1z}}{\partial l_z} \end{bmatrix} \begin{bmatrix} \frac{\partial l_x}{\partial l_0} \\ \frac{\partial l_y}{\partial l_0} \\ \frac{\partial l_z}{\partial l_0} \end{bmatrix}$$

$$= \boldsymbol{k}_{1tu,1x3} \begin{bmatrix} \frac{\partial l_x}{\partial l_0} \\ \frac{\partial l_y}{\partial l_0} \\ \frac{\partial l_z}{\partial l_0} \end{bmatrix} \tag{28}$$

e) $\boldsymbol{k}_{2fu,3x3}$ component

$$\boldsymbol{k}_{2fu,3x3} = \begin{bmatrix} \frac{\partial f_{2x}}{\partial l_x} & \frac{\partial f_{2x}}{\partial l_y} & \frac{\partial f_{2x}}{\partial l_z} \\ \frac{\partial f_{2y}}{\partial l_x} & \frac{\partial f_{2y}}{\partial l_y} & \frac{\partial f_{2y}}{\partial l_z} \\ \frac{\partial f_{2z}}{\partial l_x} & \frac{\partial f_{2z}}{\partial l_y} & \frac{\partial f_{2z}}{\partial l_z} \end{bmatrix} = -\begin{bmatrix} \frac{\partial f_{1x}}{\partial l_x} & \frac{\partial f_{1x}}{\partial l_y} & \frac{\partial f_{1x}}{\partial l_z} \\ \frac{\partial f_{1y}}{\partial l_x} & \frac{\partial f_{1y}}{\partial l_y} & \frac{\partial f_{1y}}{\partial l_z} \\ \frac{\partial f_{1z}}{\partial l_x} & \frac{\partial f_{1z}}{\partial l_y} & \frac{\partial f_{1z}}{\partial l_z} \end{bmatrix} = -\boldsymbol{k}_{1fu,3x3} \tag{29}$$

f) $\boldsymbol{k}_{2fl,3x1}$ component

$$\boldsymbol{k}_{2fl,3x1} = \begin{bmatrix} \frac{df_{2x}}{dl_0} \\ \frac{df_{2y}}{dl_0} \\ \frac{df_{2z}}{dl_0} \end{bmatrix} = -\left(\begin{bmatrix} \frac{\partial f_{1x}}{\partial l_0} \\ \frac{\partial f_{1y}}{\partial l_0} \\ \frac{\partial f_{1z}}{\partial l_0} \end{bmatrix} + \begin{bmatrix} w_x \\ w_y \\ w_z \end{bmatrix}\right) = -\left(\boldsymbol{k}_{1fl,3x1} + \begin{bmatrix} w_x \\ w_y \\ w_z \end{bmatrix}\right) \tag{30}$$

g) $\boldsymbol{k}_{2tu,1x3}$ component

$$\boldsymbol{k}_{2tu,1x3} = \begin{bmatrix} \frac{\partial T_2}{\partial l_x} & \frac{\partial T_2}{\partial l_y} & \frac{\partial T_2}{\partial l_z} \end{bmatrix} = -\begin{bmatrix} \frac{\partial T_2}{\partial f_{2x}} & \frac{\partial T_2}{\partial f_{2y}} & \frac{\partial T_2}{\partial f_{2z}} \end{bmatrix} \boldsymbol{k}_{1fu,3x3} \tag{31}$$

$$\frac{\partial T_2}{\partial f_{2i}} = \frac{f_{2i}}{T_2}, i = x, y, z \tag{32}$$

h) $\boldsymbol{k}_{2tl,1x1}$ component

$$\boldsymbol{k}_{2tl,1x1} = \frac{dT_2}{dl_0} = \begin{bmatrix} \frac{\partial T_2}{\partial f_{2x}} & \frac{\partial T_2}{\partial f_{2y}} & \frac{\partial T_2}{\partial f_{2z}} \end{bmatrix} \begin{bmatrix} \frac{\partial f_{2x}}{\partial l_0} \\ \frac{\partial f_{2y}}{\partial l_0} \\ \frac{\partial f_{2z}}{\partial l_0} \end{bmatrix} + \frac{\partial T_2}{\partial l_0} =$$

$$-\left(\begin{bmatrix} \frac{\partial T_2}{\partial f_{2x}} & \frac{\partial T_2}{\partial f_{2y}} & \frac{\partial T_2}{\partial f_{2z}} \end{bmatrix} \left(\boldsymbol{k}_{1fl,3x1} + \begin{bmatrix} w_x \\ w_y \\ w_z \end{bmatrix}\right) - \frac{\partial T_2}{\partial l_0}\right) \tag{33}$$

$$\frac{\partial T_2}{\partial l_0} = -\frac{w_1 f_4 + w_2 f_5 + w_3 f_6}{T_2} \tag{34}$$

To establish the tensile force relationship at the nodes along a sliding cable, a simple cable with three nodes and two cable segments is studied here.

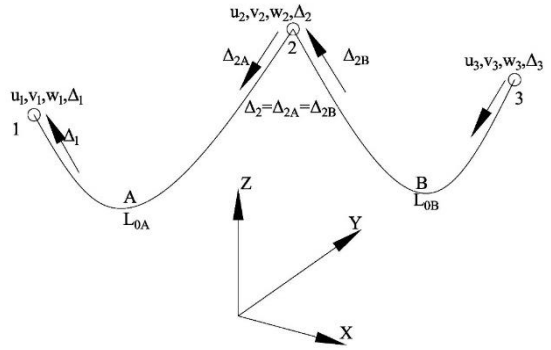

Figure 3. A Simple Sliding Catenary Cable Element with Three Nodes and Two Segments

From Figure 3, the change of the segment length can be computed as:

$$L_{0A}^{'} = L_{0A} + \Delta_{2A} - \Delta_1 \tag{35}$$

$$L_{0B}^{'} = L_{0B} + \Delta_3 - \Delta_{2B} \tag{36}$$

It should be noted that the slip distances at two side of a node should be equal. Hence,

$$\Delta_{2A} = \Delta_{2B} \tag{37}$$

The relationship of a cable segment can be determined as:

$$\begin{bmatrix} df_{1x} \\ df_{1y} \\ df_{1z} \\ df_{2x} \\ df_{2y} \\ df_{2z} \\ dT_1 \\ dT_{2A} \end{bmatrix}_{8x1} = \begin{bmatrix} -\boldsymbol{k}^A_{1fu} & \boldsymbol{k}^A_{1fu} & -\boldsymbol{k}^A_{1fl} & \boldsymbol{k}^A_{1fl} \\ -\boldsymbol{k}^A_{2fu} & \boldsymbol{k}^A_{2fu} & -\boldsymbol{k}^A_{2fl} & \boldsymbol{k}^A_{2fl} \\ -\boldsymbol{k}^A_{1tu} & \boldsymbol{k}^A_{1tu} & -\boldsymbol{k}^A_{1tl} & \boldsymbol{k}^A_{1tl} \\ -\boldsymbol{k}^A_{2tu} & \boldsymbol{k}^A_{2tu} & -\boldsymbol{k}^A_{2tl} & \boldsymbol{k}^A_{2tl} \end{bmatrix}_{8x8} \begin{bmatrix} u_1 \\ v_1 \\ w_1 \\ u_2 \\ v_2 \\ w_2 \\ \Delta_1 \\ \Delta_{2A} \end{bmatrix}_{8x1} \quad (38)$$

$$\begin{bmatrix} df_{2x} \\ df_{2y} \\ df_{2z} \\ df_{3x} \\ df_{3y} \\ df_{3z} \\ dT_{2B} \\ dT_3 \end{bmatrix}_{8x1} = \begin{bmatrix} -\boldsymbol{k}^B_{2fu} & \boldsymbol{k}^B_{2fu} & -\boldsymbol{k}^B_{2fl} & \boldsymbol{k}^B_{2fl} \\ -\boldsymbol{k}^B_{3fu} & \boldsymbol{k}^B_{3fu} & -\boldsymbol{k}^B_{3fl} & \boldsymbol{k}^B_{3fl} \\ -\boldsymbol{k}^B_{2tu} & \boldsymbol{k}^B_{2tu} & -\boldsymbol{k}^B_{2tl} & \boldsymbol{k}^B_{2tl} \\ -\boldsymbol{k}^B_{3tu} & \boldsymbol{k}^B_{3tu} & -\boldsymbol{k}^B_{3tl} & \boldsymbol{k}^B_{3tl} \end{bmatrix}_{8x8} \begin{bmatrix} u_2 \\ v_2 \\ w_2 \\ u_3 \\ v_3 \\ w_3 \\ \Delta_{2B} \\ \Delta_3 \end{bmatrix}_{8x1} \quad (39)$$

where $\boldsymbol{k}_{ifu}$, $\boldsymbol{k}_{ifl}$, $\boldsymbol{k}_{itu}$ and $\boldsymbol{k}_{itl}$ with i = 1,2,3 can be found in Eqs. (20 to 34).

Assuming that no slipping occurs at the end nodes, it has,

$$\Delta_1 = \Delta_3 = 0 \quad (40)$$

The cable tensile forces of Segment A and B at Node 2 are denoted as T_{2A} and T_{2B}, respectively. When the sliding cable is in an equilibrium state, T_{2A} should be equal to T_{2B}. Generally, the unbalanced force at Node 2 can be expressed as:

$$\Delta T_2 = T_{2A} - T_{2B} \quad (41)$$

Further, the incremental form of the unbalanced force can be derived as:

$$d\Delta T_2 = dT_{2A} - dT_{2B} \quad (42)$$

Incorporating Eqs. (38) to (42), the stiffness matrix of this sliding cable element become:

$$\begin{bmatrix} df_{1x} \\ df_{1y} \\ df_{1z} \\ df_{2x} \\ df_{2y} \\ df_{2z} \\ df_{3x} \\ df_{3y} \\ df_{3z} \\ d\Delta T_2 \end{bmatrix}_{10x1} = \begin{bmatrix} -\boldsymbol{k}^A_{1fu} & \boldsymbol{k}^A_{1fu} & 0 & \boldsymbol{k}^A_{1fl} \\ -\boldsymbol{k}^A_{2fu} & \boldsymbol{k}^A_{2fu} - \boldsymbol{k}^B_{2fu} & \boldsymbol{k}^B_{2fu} & \boldsymbol{k}^A_{2fl} - \boldsymbol{k}^B_{2fl} \\ 0 & -\boldsymbol{k}^B_{3fu} & \boldsymbol{k}^B_{3fu} & -\boldsymbol{k}^B_{3fl} \\ -\boldsymbol{k}^A_{2tu} & \boldsymbol{k}^A_{2tu} + \boldsymbol{k}^B_{2tu} & -\boldsymbol{k}^B_{2tu} & \boldsymbol{k}^A_{2tl} + \boldsymbol{k}^B_{2tl} \end{bmatrix}_{10x10} \begin{bmatrix} u_1 \\ v_1 \\ w_1 \\ u_2 \\ v_2 \\ w_2 \\ u_3 \\ v_3 \\ w_3 \\ \Delta_2 \end{bmatrix}_{10x1} \quad (43)$$

The internal force vector can be expressed by:

$$[f_{int}] = [f_{1x} \quad f_{1y} \quad f_{1z} \quad f_{2x} \quad f_{2y} \quad f_{2z} \quad f_{3x} \quad f_{3y} \quad f_{3z} \quad T_{2A} - T_{2B}]^T \quad (44)$$

As the tensile forces at Node 2 from both segments should be finally in the equilibrium state, the external force vector can be given by:

$$[F_{ext}] = [F_{1x} \quad F_{1y} \quad F_{1z} \quad F_{2x} \quad F_{2y} \quad F_{2z} \quad F_{3x} \quad F_{3y} \quad F_{3z} \quad 0]^T \quad (45)$$

Repeating the above procedure, the stiffness matrix of the sliding cable with three nodes and two segments can be extended to the sliding cable with N nodes and N-1 segments.

4. Verification examples

Several examples from the literature are used to verify the capability and accuracy of the proposed sliding cable element.

4.1. Single cable under point load

The first example studies a simple structure with one single span suspended cable. The cable spans 304.8 m with two end supports at the same level. Initially, the sag at the mid-span is 30.48 m. A concentrated load is applied to the cable located at the node which is 121.92 m away from the center in the horizontal direction. The material and geometry parameters of the cable are summarized in Table 1. Both the conventional catenary cable element and the proposed sliding cable element are used to study this example.

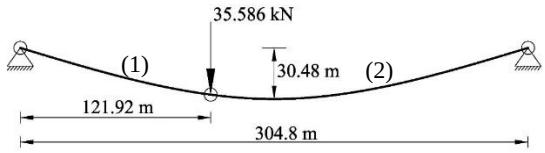

Figure 4. Single Span Suspended Cable Structure

The displacement of the loaded point is computed from the initial configuration. This example has been analyzed by other researchers using different methods. The analysis results can be found in literature and are compared with the results from the proposed element. The initial and deformed shapes are shown in Figure 5.

Table 1
Parameters of the Cable under Concentrated Load

Parameter	Value
Cross sectional area, A_0	548.4 mm^2
Elastic modulus, E	131.0 kN/mm^2
Cable selfweight, q_0	46.12 N/m
Cable length, L	312.73 m
Length of first segment, L_1	125.88 m
Length of second segment, L_2	186.85 m

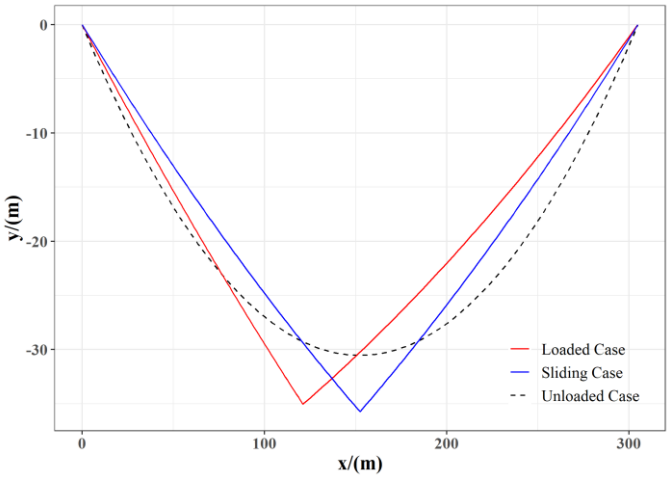

Figure 5. Initial and Deformed Shape of Single Suspended Cable Structure

Table 2 summarizes the results obtained from the literature. It can be seen that the displacements from this paper are in good agreement with others.

Table 2
Results for the Cable under Concentrated Load

Reference	Element type	Horizontal displacement (m)	Vertical displacement (m)
Jayaraman and Knudson (1981)	Elastic catenary	-0.859	-5.626
Andreu et al. (2006)	Elastic catenary	-0.860	-5.626
Yang & Tsay (2007)	Elastic catenary	-0.859	-5.625
Thai and Kim (2011)	Elastic catenary	-0.859	-5.626
Salehi Ahmad Abad et al. (2013)	Elastic catenary	-0.859	-5.626
Crusells-Girona et al. (2017)	Discrete elastic catenary	-0.861	-5.630
Present work	Elastic catenary	-0.852	-5.764

Note that the sliding behavior along the cable is not considered in the above study. In reality, the loading point may move in the leftward and downward directions due to unbalanced force at the two sides of the point. The deformed

shape of the cable is plotted in Figure 5. As there are no external lateral forces applied to the point, the unbalanced horizontal component of cable force will move the point to a new position and finally achieve an equilibrium state. Clearly, the final position is at the mid-span in this example. The deformed shape of the cable in this case is also shown in Figure 5. The tension forces of the cable segments at the loaded node are summarized in Table 3 in both cases.

Table 3
Tensile forces of the cable under concentrated load

Case	Segment	Tensile force (L) /(kN)	Tensile force (R) /(kN)
No sliding effect	(1)	100.102	98.488
	(2)	96.347	97.961
With sliding effect	(1)	94.593	92.947
	(2)	92.947	94.593

From Table 3, significant difference is found between the cases with and without sliding effect at the loading point. When using the traditional catenary cable element without sliding effect, the axial forces on both sides of the loaded node are not equal. When considering the sliding effect, the continuity of the cable tension force will be ensured during the analysis by adjusting the segment length of the cable. Generally speaking, the sliding behavior may help the cable structures to find a optimal position to resist the external loads.

4.2. Single cable sliding along one support

The second example examines the sliding effect of a single the cable passing through one intermediate support as shown in Figure 6. The cable segments are 8.0 m and 12.0 m, respectively. The initial unstressed lengths of the cable are 8.02 m and 12.02 m. The material properties, geometric dimensions and loadings are summarized in Table 4. The cable self-weight per unit length q_0 is 0.2 kN/m. The elastic modulus E and the cross-sectional area A_0 are 1.7 x 10^5 MPa and 6.74 x 10^{-5} m^2 respectively. Distributed loading of 0.3 kN/m and 0.8 kN/m are applied to the first and the second spans respectively.

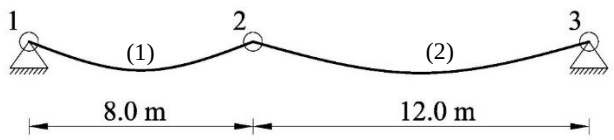

Figure 6. Single Cable Sliding along One Support

Table 4
Parameters of the Single Cable Sliding along One Support

Parameter	Value
Cable selfweight, q_0	0.2 kN/m
Elastic modulus, E	1.7 x 10^5 MPa
Cross-sectional Area, A_0	6.74 x 10^{-5} m^2
Distributed load in the first span, q_1	0.3 kN/m
Distibuted load in the second span, q_2	0.8 kN/m

Table 5 lists the tension forces of the cable under self-weight and the external distributed loads. Also, the cases with and without sliding effect are taken into account. The results from the proposed method are shown in Table 5 against with Nie et al. (2003) . It can be seen that the present work agrees well with with Nie et al. (2003) considering both cases.

Table 5
Tensile Forces of the Single Cable Sliding along One Support

Reference	Sliding	Segment	Horizontal force / kN	Tensile force (L) / kN	Tensile force (R) / kN
Nie et al. (2003)	Yes	(1)	8.310	8.349	8.349
		(2)	8.262	8.349	8.349
	No	(1)	5.941	5.995	5.995
		(2)	9.752	9.825	9.825
Present work	Yes	(1)	8.305	8.344	8.344
		(2)	8.256	8.344	8.344
	No	(1)	5.941	5.995	5.995
		(2)	9.752	9.826	9.826

Similarly, the results with sliding effect are different from the case without sliding effect. The deformed shapes for the two cases from this study are plotted in Fingure 7. Thus, if the clamp at the intermediate support allows the cable passing through the support, the analysis model should take this effect into account.

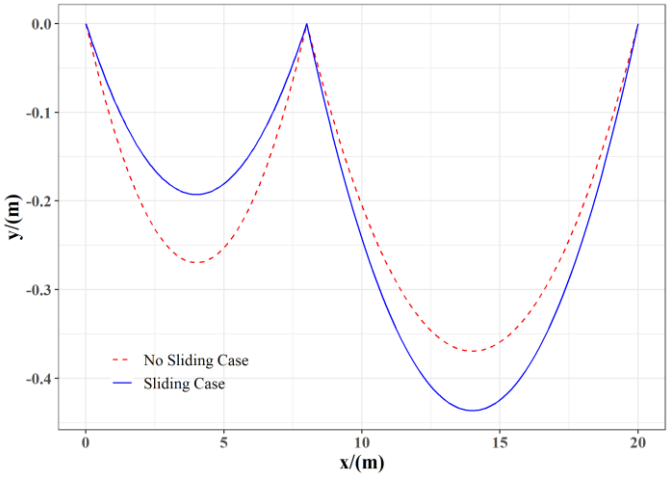

Figure 7. Deformed Shape of the Single Cable Sliding along One Support

4.3. Single cable sliding along two supports at diffferent levels

This example studies a single cable with two intermediate supports at different levels as shown in Figure 8. The material properties and the cross-sectional area are same as the section example and can be referred to Table 4. However, the distributed loads on the cable segments are 0.8 kN/m, 1.8 kN/m, and 2.8 kN/m, respectively in this example.

The results from the proposed sliding element against the results from literature are shown in Table 6. The deformed shapes with and without consideration of sliding effect from this study are plotted in Fingure 9.

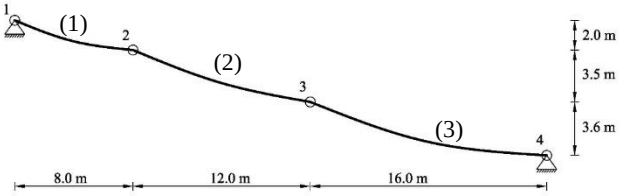

Figure 8. Single Cable Sliding along Two Supports at Diffferent Levels

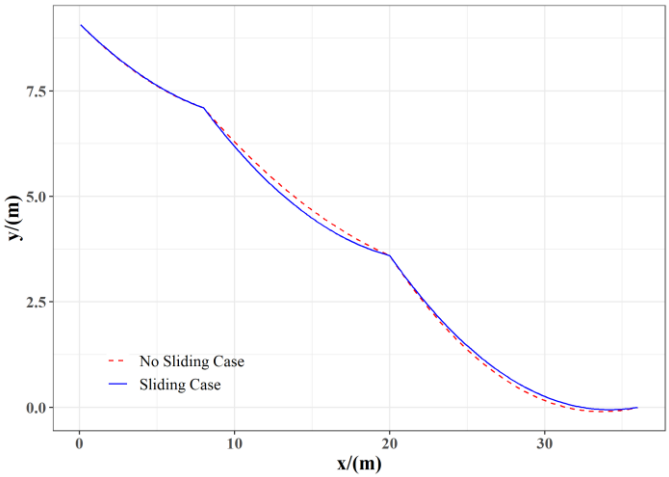

Figure 9. Deformed Shape of the Single Cable Sliding along Two Supports

In general, the results using the proposed cable element show in good agreement with others. It demonstrates the relibility and accuracy of the proposed method. Note that only one cable element with several internal nodes is used to simulate the cable structure. It also shows that the proposed method can be applied to multi-node cable allowing for sliding effect.

Table 6
Tensile Forces of the Single Cable Sliding along Two Supports

Reference	Segment	Length / m	Horizontal force / kN	Tensile force (L) / kN	Tensile force (R) / kN
Nie et al. (2003)	(1)	-	7.017	7.479	7.079
	(2)	-	6.350	7.079	6.379
	(3)	-	5.649	6.379	5.660
Wei (2006)	(1)	8.257	7.017	7.479	7.079
	(2)	12.563	6.349	7.079	6.379
	(3)	16.600	5.649	6.379	5.660
Present work	(1)	8.257	7.017	7.479	7.079
	(2)	12.563	6.349	7.079	6.379
	(3)	16.600	5.649	6.379	5.660

4.4. Transport pulley system

This example investigates the stability of a cable supported by a pulley. In this structure, the cable is anchored at both ends with a level difference of 50 m. A pulley roller is assigned to the structure at a level of 50 m higher than the right support as shown in Figure 10. The cable is continuous and therefore it can slide at the roller position. This example is to determine the equilibrium state of the structure since the roller can move freely along the horizontal direction. The final position of the roller and the segment lengths of the cable in the equilibrium states will be found through the nonlinear analysis. For simplicity, the roller radius as well as the friction is ignored in this example. The parameters for nonlinear analysis are listed in Table 7.

Table 7
Parameters of the Transport Pulley System

Parameter	Value
Cable selfweight, q_0	62.0679 N/m
Elastic modulus, E	1.6 x 10^4 MPa
Cross-sectional Area, A_0	8.05 x 10^{-4} m^2
Cable length, L	500 m

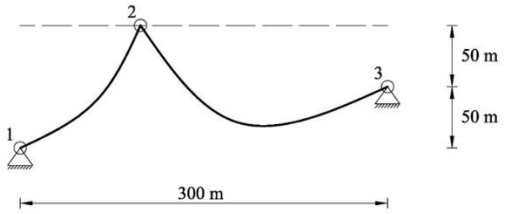

Figure 10. Configuration of the Structure in Example 3

The initial position of the roller is assumed to be located at the leftmost position while the initial length of the left segment is assumed to be the span length between the left support and the roller. The movement of the roller and the length adjustment are the two variables in the analysis.

The first equilibrium state is achieved when the roller reaches the point with a horizontal distance of 47.25m from the leftmost position. The lengths of the left and right segments are 110.83 and 389.17 m by using the proposed slidable element, respectively.

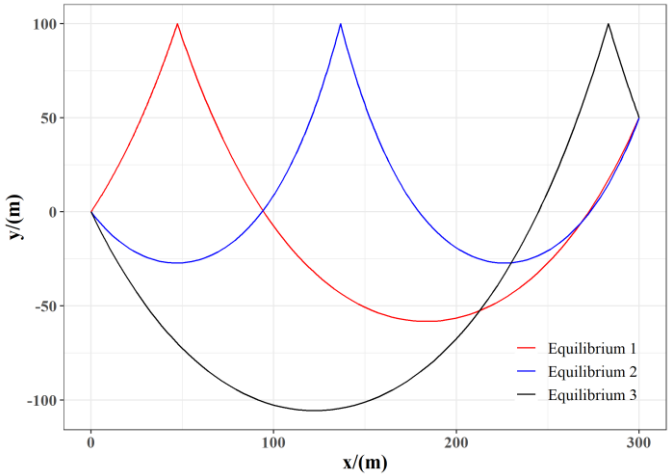

Figure 11. Equilibrium States of the Transport Pulley System

The second equilibrium position of the roller locates at the position that is 136.535 m from the left end node. The third equilibrium state is achieved when the roller is initially positioned at the right most of the line. The initial length of the second segment is the span length of the roller and the end node which is 50 m in this case. The analysis results of this structure including the unstrained length of the left segment as well as the tensile force at the roller are summarized in **Table 8**. In addition, the results conducted by other researchers are also collected for comparison. It can be seen that the results from current work agree well with others.

Table 8
Results of the Planar Transport Pulley System

Reference	l_1 (m)	T_1(kN)	l_2 (m)	T_2(kN)	l_3 (m)	T_3(kN)
Bruno & Leonardi (1999)	111.07	15.499	-	-	446.37	17.952
Such et al. (2009)	110.96	14.531	-	-	446.92	17.966
Impollonia et al. (2011)	110.83	14.531	221.52	10.631	447.30	17.982
Crusells-Girona et al. (2017) (continuous)	110.83	4.709-14.514	221.53	2.726-10.622	447.30	5.222-17.96
Crusells-Girona et al. (2017) (discontinuous)	110.83	4.709-14.515	221.51	2.726-10.622	447.29	5.222-17.957
Present work	110.83	14.516	221.52	10.620	447.29	17.963

The planar pulley system is also extended to a spatial one. The sliding line of the pulley is positioned at 50 m from the plan of the two end nodes. The length of the cable is 500 m. The pulley slides along the new line. The equilibrium configurations are detected based on the new geometric setting of the system. The analysis results are listed in Table 9. Again, the results from this study are close to Impollonia et al. (2011).

Table 9
Results of the Spatial Transport Pulley System

Reference	l_1 (m)	T_1(kN)	l_2 (m)	T_2(kN)	l_3 (m)	T_3(kN)
Impollonia et al. (2011)	126.122	14.3966	219.983	10.994	424.757	17.753
Present work	126.122	14.109	219.983	10.774	424.757	17.398

5. Conclusions

Cable structures have been extensively used due to light weight but with high strength. Also, the cables can cater for complex structural forms with optimal load paths via large deflection. These features make them applicable in many structures such as flexible barriers, transmission lines, pulley systems, suspend-dome structures, clustered tensegrity and parachute systems. However, sliding motion is generally observed and particular concerns should be taken in the design of cable structures. The risk of sliding in some cable structures should be evaluated. On the contrary, engineers can take the benefit of sliding behavior to develop the innovative cable systems like flexible barriers to absort large impact energy.

The conventional analysis methods need many straight-line cable elements but with inaccurate results and low numerical efficiency. The well-known catenary cable element show high performance in the cable structures but limited to no sliding cases. Thus, an advanced cable element allowing for sliding effect is urgently required in the practical analysis of cable structures.

In this paper, a super cable element based on the conventional catenary cable element is proposed to model the segments within a slidable cable. In the proposed super element, every segment performs in the characteristic of catenary cable. Meanwhile, the sliding motion will be activated when the unbalanced axial force between segments are deteced and as a result, the sliding behaviours of the cables in both taut and slack states can be modelled. This work has not been done in previous research and the proposed element can be applied to many structures. The verification examples show the accuracy and efficiency of the proposed element in the analysis of cable structures with internal movement passing the supports or relocation of the loading points.

Acknowledgments

The authors are grateful for financial support from the Research Grant Council of the Hong Kong SAR Government on the project “Joint-based second order direct analysis for domed structures allowing for finite joint stiffness (PolyU 152039/18E)”, “Second-order analysis and design of scaffolds with scissor braces and allowing for kink imperfections (PolyU 152035/20E)” and Innovation and Technology Fund for the project “A new membrane-flood gate system for extreme weather hazardous mitigations for use in Hong Kong and worldwide (K-ZPD1)”.

Referernce

1. Andreu, A., Gil, L., & Roca, P. (2006). A new deformable catenary element for the analysis of cable net structures. Computers & Structures, 84(29-30), 1882-1890. https://doi.org/10.1016/J.COMPSTRUC.2006.08.021
2. Aufaure, M. (1993). A finite element of cable passing through a pulley. Computers & Structures, 46(5), 807-812. https://doi.org/10.1016/0045-7949(93)90143-2
3. Aufaure, M. (2000). A three-node cable element ensuring the continuity of the horizontal tension; a clamp–cable element. Computers & Structures, 74(2), 243-251. https://doi.org/10.1016/S0045-7949(99)00015-2
4. Bruno, D., & Leonardi, A. (1999). Nonlinear structural models in cableway transport systems. Simulation Practice and Theory, 7(3), 207-218. https://doi.org/10.1016/S0928-4869(98)00024-X
5. Chen, Z. H., Wu, Y. J., Yin, Y., & Shan, C. (2010). Formulation and application of multi-node sliding cable element for the analysis of Suspen-Dome structures. Finite Elements in Analysis and Design, 46(9), 743-750. https://doi.org/10.1016/J.FINEL.2010.04.003
6. Coulibaly, J. B., Chanut, M.-A., Lambert, S., & Nicot, F. (2018). Sliding cable modeling: An attempt at a unified formulation. International Journal of Solids and Structures, 130-131, 1-10. https://doi.org/10.1016/J.IJSOLSTR.2017.10.025
7. Crusells-Girona, M., Filippou, F. C., & Taylor, R. L. (2017). A mixed formulation for nonlinear analysis of cable structures. Computers & Structures, 186, 50-61. https://doi.org/10.1016/J.COMPSTRUC.2017.03.011
8. Impollonia, N., Ricciardi, G., & Saitta, F. (2011). Statics of elastic cables under 3D point forces. International Journal of Solids and Structures, 48(9), 1268-1276. https://doi.org/10.1016/J.IJSOLSTR.2011.01.007
9. Jayaraman, H. B., & Knudson, W. C. (1981). A curved element for the analysis of cable structures. Computers & Structures, 14(3-4), 325-333. https://doi.org/10.1016/0045-7949(81)90016-X
10. Ju, F., & Choo, Y. S. (2005). Super element approach to cable passing through multiple pulleys. International Journal of Solids and Structures, 42(11-12), 3533-3547. https://doi.org/10.1016/J.IJSOLSTR.2004.10.014
11. Kan, Z., Peng, H., Chen, B., & Zhong, W. (2018). A sliding cable element of multibody dynamics with application to nonlinear dynamic deployment analysis of clustered tensegrity. International Journal of Solids and Structures, 130, 61-79.
12. LSTC. (2019). LS-DYNA Theory Manual. In: Livermore Software Technology Corporation.
13. Nie, J.-g., Chen, B.-l., & Xiao, J.-c. (2003). Nonlinear static analysis of continuous cables with sliding at the middle supportings. Jisuan Lixue Xuebao(Chinese Journal of Computational Mechanics)(China), 20(3), 320-324.
14. Salehi Ahmad Abad, M., Shooshtari, A., Esmaeili, V., & Naghavi Riabi, A. (2013). Nonlinear analysis of cable structures under general loadings. Finite Elements in Analysis and Design, 73, 11-19. https://doi.org/10.1016/j.finel.2013.05.002
15. Such, M., Jimenez-Octavio, J. R., Carnicero, A., & Lopez-Garcia, O. (2009). An approach based on the catenary equation to deal with static analysis of three dimensional cable structures. Engineering Structures, 31(9), 2162-2170. https://doi.org/10.1016/J.ENGSTRUCT.2009.03.018
16. Thai, H.-T., & Kim, S.-E. (2011). Nonlinear static and dynamic analysis of cable structures. Finite Elements in Analysis and Design, 47(3), 237-246. https://doi.org/10.1016/J.FINEL.2010.10.005
17. Wei, J. D. (2006). Friction sliding cable element for structural analysis of prestressed steel truss. Chinese Journal of Computational Mechanics, 23(6), 800-806.
18. Yang, Y. B., & Tsay, J.-Y. (2007). Geometric nonlinear analysis of cable structures with a two-node cable element by generalized displacement control method. International Journal of Structural Stability and Dynamics, 07(04), 571-588. https://doi.org/10.1142/S0219455407002435
19. Yu, Z., Qiao, Y., Zhao, L., Xu, H., Zhao, S., & Liu, Y. (2018). A Simple Analytical Method for Evaluation of Flexible Rockfall Barrier Part 1: Working Mechanism and Analytical Solution. Advanced Steel Construction, 14(2), 115-141. https://doi.org/10.18057/IJASC.2018.14.2.1
20. Zhao, L., He, J. W., Yu, Z. X., Liu, Y. P., Zhou, Z. H., & Chan, S. L. (2020). Coupled numerical simulation of a flexible barrier impacted by debris flow with boulders in front. Landslides. https://doi.org/10.1007/s10346-020-01463-x
21. Zhao, L., Yu, Z.-X., Liu, Y.-P., He, J.-W., Chan, S.-L., & Zhao, S.-C. (2020). Numerical simulation of responses of flexible rockfall barriers under impact loading at different positions. Journal of Constructional Steel Research, 167, 105953. https://doi.org/10.1016/J.JCSR.2020.105953
22. Zhou, B., Accorsi, M. L., & Leonard, J. W. (2004). Finite element formulation for modeling sliding cable elements. Computers and Structures. https://doi.org/10.1016/j.compstruc.2003.08.006